Review of Inductance Identification Methods Considering Inverter Nonlinearity for PMSM*

Qiwei Wang[1], *Jiqing Xue*[1], *Gaolin Wang*[1*], *Yihua Hu*[2] *and Dianguo Xu*[1]
(1. School of Electrical Engineering and Automation, Harbin Institute of Technology, Harbin 150000, China;
2. Department of Engineering, King's College London, London WC2R 2LS, UK)

Abstract: Permanent magnet synchronous motors (PMSMs) are widely used in high-power-density and flexible control methods. Generally, the inductance changes significantly in real-time machine operations because of magnetic saturation and coupling effects. Therefore, the identification of inductance is crucial for PMSM control. Existing inductance identification methods are primarily based on the voltage source inverter (VSI), making inverter nonlinearity one of the main error sources in inductance identification. To improve the accuracy of inductance identification, it is necessary to compensate for the inverter nonlinearity effect. In this study, an overview of the PMSM inductance identification and the related inverter nonlinearity self-learning methods are presented.

Keywords: Inductance identification, inverter nonlinearity self-learning, permanent magnet synchronous motor

1 Introduction

Permanent magnet synchronous motors (PMSMs) are widely used in the industrial field because of their high torque and power density [1-2]. The high-performance control methods of PMSM primarily rely on accurate parameters, among which the inductance generally changes significantly during motor operation owing to magnetic saturation and coupling saturation effects [3]. Hence, inductance identification is crucial for PMSM control such as sensorless control [4-5], deadbeat control [6-7], and model predictive control (MPC) [8-9]. The inductance can also be applied to the status detection and fault diagnosis of PMSM.

In traditional motor-control strategies, the inductance is usually assumed to be constant. However, in actual PMSM control, the stator current changes under different operating conditions, causing magnetic saturation and cross-saturation effects, and further changing the inductance [10]. PMSM control methods with high accuracy and performance have attracted increasing attention because inductance identification strategies are required [11]. In early research, inductance identification was performed using detection devices, which increased the cost and reduced generality. Simultaneously, the detection devices can only be used offline. The effects of magnetic saturation on the inductance cannot be considered. To solve these problems, the identification achieved by the controller has been investigated over the past decade.

Currently, VSI-based controllers are commonly used in PMSM control systems, making the inductance identification method more realizable and practical under various operation conditions [12]. However, because a VSI-based controller is not an ideal device, inverter nonlinearity causes voltage errors in the motor control, which also has an adverse impact on inductance identification [12-13]. The inverter nonlinearity effect contains many error factors such as the dead time effect, parasitic capacitance effect, and voltage drop of the switching device [14]. In recent years, studies on inverter nonlinearity estimation and compensation have been conducted to further improve inductance identification accuracy.

This paper presents a comprehensive discussion of the existing research on PMSM inductance identification and related inverter nonlinearity compensation. This paper is organized as follows. In Section 2, the characteristics of the inductance and inverter nonlinearity under VSI-based drives are introduced. PMSM inductance identification technologies are presented in Section 3. The inverter

Manuscript received July 29, 2023; revised October 9, 2023; accepted October 23, 2023. Date of publication June 30, 2024; date of current version November 10, 2023.
* Corresponding Author, E-mail: WGL818@hit.edu.cn
* Supported by the National Natural Science Foundation of China (52307048) and the Postdoctoral General Foundation of Heilongjiang (LBH-Z23022).
Digital Object Identifier: 10.23919/CJEE.2023.000046

nonlinearity self-learning and compensation methods are presented in Section 4. Section 5 discusses future trends and concludes the paper.

2 Inductance and inverter nonlinearity models in VSI-based PMSM drive

In this section, the saturation characteristics of the inductance are analyzed under different operating conditions along with the rank deficiency in the identification process. Furthermore, the inverter nonlinearity effect in the inductance identification is introduced.

2.1 Saturation effect of inductance

Owing to the saturation characteristics of the magnetic material of the yokes, a magnetic saturation effect occurs during actual motor operation [10]. According to the magnetization curve of ferromagnetic materials, with an increase in the magnetic field, the flux linkage simultaneously increases, which reduces the magnetic permeability and inductance [2]. The simulation results for the magnetic saturation effects of the PMSM are shown in Fig. 1, wherein i_n represents the rated value of the current.

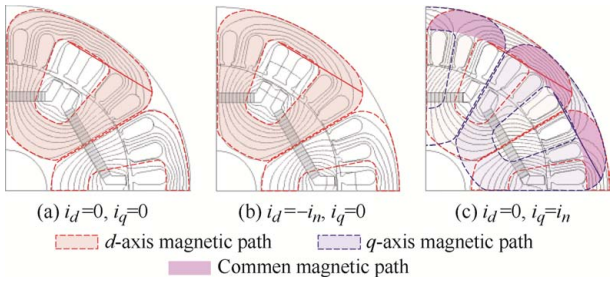

Fig. 1 Simulation results of magnetic saturation of PMSM in different working conditions

The density of magnetic lines represents the degree of saturation. As shown in Figs. 1a-1b, the magnetization and demagnetization currents in the PMSM increase and weaken the degree of magnetic saturation, respectively, which is defined as the magnetic saturation effect. As shown in Fig. 1c, a common magnetic path exists between *dq*-axis magnetic circuits, causing a cross-saturation effect, where the inductance is affected by both *dq*-axis currents.

2.2 Inductance identification models

As the *dq*-axis model is generally applied to PMSM control, *dq*-axis inductances are the identification targets. The *dq*-axis voltage equations are the most commonly used identification models and are expressed as follows

$$\begin{cases} u_d = R_s i_d + L_{d\_inc}\dfrac{\mathrm{d}i_d}{\mathrm{d}t} - \omega_e L_{q\_app} i_q \\ u_q = R_s i_q + L_{q\_inc}\dfrac{\mathrm{d}i_q}{\mathrm{d}t} + \omega_e L_{d\_app} i_d + \omega_e \psi_f \end{cases} \tag{1}$$

where $u_{d,q}$ denote the *dq*-axis voltages, $i_{d,q}$ denote the *dq*-axis currents, R_s denotes the stator resistance, and ω_e signifies the rotational speed. L_{d,q_inc} and L_{d,q_app} denote the incremental and apparent inductances in *dq*-axes, respectively [15]. Considering the magnetic and cross-saturation effects, L_{d,q_inc} and L_{d,q_app} are different. However, L_{d,q_inc} and L_{d,q_app} are mathematically equal, and their expressions are as follows

$$L_{x\_inc} = \frac{\mathrm{d}(L_{x\_app} i_x)}{\mathrm{d}i_x} \quad x = d, q \tag{2}$$

Among the existing inductance identification methods, the methods based on steady voltage models achieve L_{d,q_app} identification, while the methods based on transient voltage models achieve L_{d,q_inc} identification [16-17]. In conventional inductance identification methods, the number of unknown variables exceeds that of the model equations. Hence, a rank deficiency occurs during the inductance identification process, which is a core problem that must be solved.

Except for the *dq*-axis voltage equations, some inductance identification strategies are based on other models, such as *αβ*-axis model [18]. These methods can be transformed into a *dq*-axis model based method via a coordination transformation. Furthermore, regardless of the applied model, the rank deficiency problem should always be considered.

2.3 Inverter nonlinearity effects

It is known that the VSI-based drive is not ideal, as the physical properties and drive strategies lead to inverter nonlinearity effects, including the parasitic capacitance effect [19], dead time effect [20], voltage drop, and switching delay of switching devices [21]. The overall effect of the inverter nonlinearity on the output voltage is shown in Fig. 2. The parasitic capacitance effect exists mainly in the relatively low current region, whereas the dead time effect exists in the full current region [22].

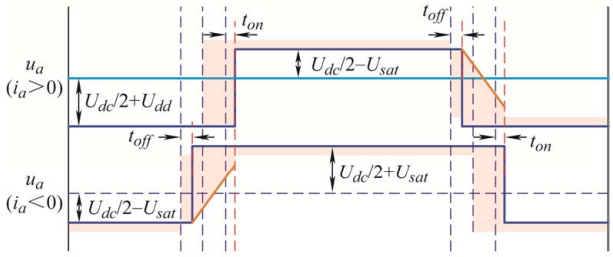

t_d-Dead time t_{on}, t_{off}-Switching delay of switching devices
U_{dc}-DC bus voltage U_{sat}-Voltage drop of switching devices
The shadow: Voltage error caused by inverter nonlinearity effect

Fig. 2 Diagram of inverter nonlinearity effects

The inverter nonlinearity causes an error between the voltage command and output voltage, which reduces the control efficiency, especially under low-speed and light-load conditions [23-24]. The error between the reference voltage and the output voltage caused by inverter nonlinearity can be expressed as

$$u_x(i_x)=R_s i_x+u_{xinv}(i_x) \quad x=a,b,c \tag{3}$$

where u_{abcinv} is the nonlinear voltage of the inverter in the *abc* phases. The voltages are generally required in the inductance identification, which makes inverter nonlinearity a problem that must be addressed [13, 25].

Owing to the absence of a phase delay between the current and error voltage of the inverter nonlinearity, the inverter nonlinearity error can be regarded as an equivalent resistance [14, 26]. As illustrated in Fig. 3, in Region 1, the inverter nonlinearity error voltage is nonlinear in the low-current region, where the equivalent resistance is large. When the current exceeds a certain value, the inverter nonlinearity error voltage is constant, and the dead-time effect, switch device voltage drop, and turn-on/off delay are the major components of the inverter nonlinearity effect, as shown in Fig. 3, Region 2. In the absence of a parasitic capacitance effect, the inverter nonlinear error voltage acts as a sign function of the current.

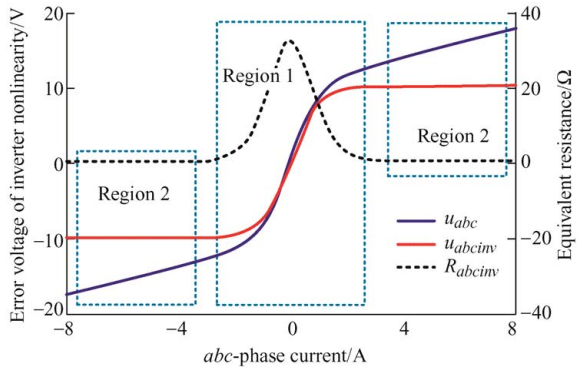

Fig. 3 *abc*-phase inverter nonlinear voltage error and equivalent resistance

3 Inductance identification of PMSM

This section reviews conventional inductance identification methods. The aforementioned methods are classified into different categories based on application conditions (offline and online), a comparison of which is presented in Tab. 1. In actual motor operation, the inductances of the PMSM change under different operating conditions, as illustrated in Fig. 4.

Tab. 1 Comparison of offline and online inductance identification methods

Contrastive items	Offline identification methods	Online identification methods
Applicable state	Offline condition with rotor standstill	Different online operation conditions
Identification purpose	Auto-tuning for machine start up and machine control	Self-commissioning; Health state detection; Fault diagnosis
Signal injection type	HF signal injection for signal excitation	HF/offset signal injection for solving rank deficiency
Signal injection effectiveness	Don't consume online control resources; Don't affect online control process	Consume online resources; Affect online control process
Identification practicality	Hard to simulate actual online machine states; Data storage requirement	Identification under real-time machine states; No data storage requirement

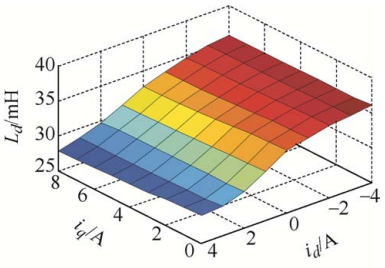

(a) L_d under different $i_{d,q}$ combinations

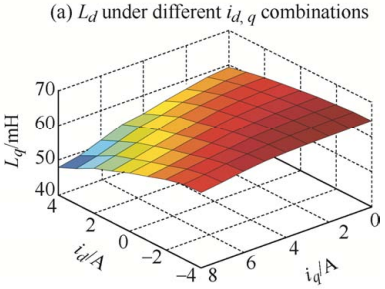

(b) L_q under different $i_{d,q}$ combinations

Fig. 4 Inductance surfaces for different $i_{d,q}$ combinations

3.1 Offline inductance identification

As there is no current in the PMSM under offline conditions, offline inductance identification can be achieved using signal injection strategies. Based on the injected signals, conventional identification methods can be divided into square-wave and sine-wave

injection methods.

3.1.1 Square wave injection based methods

The square-wave-injection-based method is the most commonly used offline inductance identification strategy. The injected voltage and the induced current are first applied to achieve the flux linkage estimation, and then the *dq*-axis inductances are calculated by the differential operations of the flux linkage [27-29]. The corresponding mathematical equations and block diagrams are presented in Eq. (4) and Fig. 5.

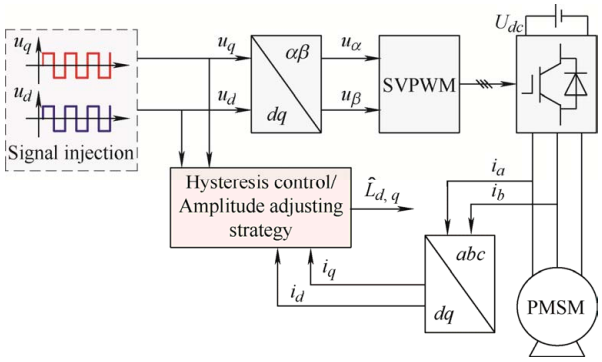

Fig. 5 Block diagram of offline inductance identification strategy based on square-wave signal injection

$$\begin{cases}\psi_x(i_x)=\int\left(u_x(i_x)-R_s i_x\right)\mathrm{d}t \\ L_x(i_x)=\Delta\psi_x/\Delta i_x\end{cases} \quad x=d,q \tag{4}$$

where $\psi_{d,q}$ denote the *dq*-axis flux linkages. An inductance identification strategy based on *dq*-axis square wave injection was proposed in Ref. [28], where the amplitude and frequency of the injected voltages can be adjusted by hysteresis control. The linear least-squares algorithm was used to improve the identification accuracy. In Ref. [30], the square wave injection method was proposed with the rotor position closed-loop tracked so that the rotation of the rotor during the signal injection process could be obtained without the encoder, improving the stability of the proposed identification method. In Ref. [29], a flux saturation approximation function was introduced to simplify the inductance identification procedure with *dq*-axis square wave signal injection, where the identification accuracy was verified by the maximum torque per ampere algorithm.

High-frequency (HF) square-wave voltage injection into a two-phase rotating coordinate system was proposed in Ref. [31]. The *dq*-axis inductances can be extracted from the HF (HF) response currents under both offline and online conditions, improving the universality of the algorithm. By increasing the injection frequency of the square wave, the injected signal becomes a pulse wave that can be used for inductance identification. An inductance identification method based on double-direction pulse signal injection under a rotating shaft system was presented, in which no additional auxiliary equipment was required [32].

The square-wave injection-based offline inductance identification method considers the saturation effects of the inductance by adjusting the injection amplitude.

3.1.2 Sine wave injection based methods

Recently, the offline inductance identification method based on sine-wave injection has drawn increasing attention; its diagram is shown in Fig. 6. The inductance can be calculated using the frequency and amplitude of the injected signals, as shown in Eq. (5). These methods can be further divided into several different categories based on signal injection strategies [33].

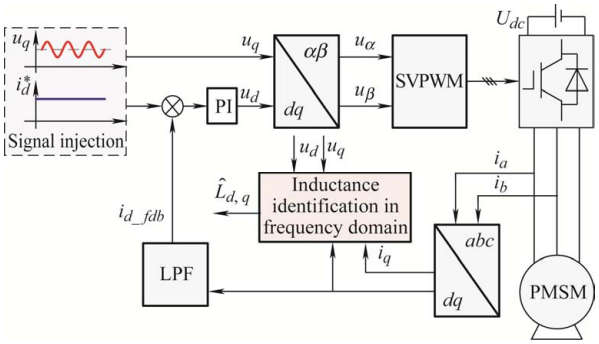

Fig. 6 Block diagram of offline inductance identification strategy based on sine wave injection

The *dq*-axis sine wave signal injection method is first investigated. In Ref. [26], an injection method with *dq*-axis HF sinusoidal voltage injection was proposed, in which the inductance was estimated based on the information of the injected voltage and induced current. To prevent rotor rotation during the identification process, a *d*-axis current bias is applied to fix the rotor position. In Ref. [33], the DC square wave and AC sine wave combination signal injection method was applied with or without rotor locking, which realizes inductance estimation considering the magnetic saturation and cross-saturation effects. In Ref. [34], the DC and AC combination signal injection

method was further investigated, where the injection amplitude and frequency were selected to improve identification effectiveness.

To deal with the inverter nonlinearity effect, the double-amplitude injection method [35] and the double-frequency double-amplitude injection method [12] based on HF injection have been proposed. In addition to the *dq*-axis signal injection methods, other signal injection strategies with different injection axes or mixed signal injection have also been proposed to satisfy different application conditions. In Ref. [36], an offline inductance identification strategy was proposed with sinusoidal voltage injection at different rotor positions. The *dq*-axis inductance can be obtained from a spatial inductance map.

$$\begin{cases} u_{xh}=\mathrm{Re}[U_{xh}\exp(j(\omega_{xh}t+\theta_{ud}))] \\ i_{xh}=\mathrm{Re}[I_{xh}\exp(j(\omega_{xh}t+\theta_{id}))] \\ L_x=\mathrm{Im}\left[\dfrac{u_{xh}}{\omega_x i_{xh}}\right]=\dfrac{U_{xh}}{\omega_x I_{xh}}\sin(\theta_{xu}-\theta_{xi}) \end{cases} \quad x=d,q \qquad (5)$$

where $u_{d,qh}$ and $i_{d,qh}$ represent the injected *d*- and *q*-axis HF voltages and currents, respectively. $U_{d,qh}$ and $I_{d,qh}$ denote the amplitudes of the injected *dq*-axis voltage and current, respectively. Re[] and Im[] represent the real and imaginary parts, respectively. $\theta_{d,qu}$ and $\theta_{d,qi}$ represent the initial phase angles of the HF voltage and current. $\omega_{d,qh}$ denote the injected *dq*-axis angular frequencies. This type of method is immune to inverter nonlinearity by avoiding the influence of the equivalent resistance.

To consider the saturation effects of inductance, different PMSM saturation conditions must be simulated offline [2]. To satisfy this requirement, the injected signals must be adjusted several times to create different *dq*-axis current conditions where the inductance is identified and sampled simultaneously [30]. In this case, the complexity of the data computation and storage is inevitably increased [26, 37]. To solve these problems, data fitting and interpolation strategies have been proposed [15, 38]. Considering the applied *dq*-axis signal injection, most conventional offline methods require an accurate *dq*-axis position. Hence, encoder or sensorless control is essential [33-34]. Furthermore, the injected signal may cause motor rotation, which affects the identification accuracy. To address this problem, motor stability during signal injection has been analyzed, and modified signal injection schemes have been proposed [28, 30].

When motor rotation is allowed, the inductance can also be identified under the free rotation state in the offline condition. In Ref. [39], by providing *dq* current reference values, the *dq*-axis flux linkage versus current curves could be identified under the PMSM free rotation state. The *dq*-axis inductances can be calculated using the *dq*-axis flux linkages.

Existing offline inductance identification methods are based on PMSM voltage equations, where the output voltage is affected by the inverter nonlinearity effect. Hence, inverter nonlinearity should be compensated in the offline inductance identification process [40-42]. A comparison of widely used offline methods is presented in Tab. 2.

Tab. 2 Comparison of widely applied offline inductance identification methods

Contrastive items	Method in Ref. [30]	Method in Ref. [33]	Method in Ref. [34]	Method in Ref. [38]
Signal injection	Square wave	Sine wave	Sine wave & DC current	HF Sine wave & DC current
Inverter nonlinearity effect	Affected by inverter error	Affected by inverter error	Affected by inverter error	Immune to inverter error
Allowable identification range	Limited $i_{d,q}$ range	Limited $i_{d,q}$ range	Full $i_{d,q}$ range (with locked rotor)	Full $i_{d,q}$ range (with locked rotor)

3.2 Online inductance identification

Although offline methods have made significant progress in inductance identification, they cannot fully simulate the actual online PMSM saturation conditions. Online inductance identification methods have received increasing attention for further improving inductance identification technology.

3.2.1 Steady-state voltage equation based methods

The steady-state voltage equations are commonly used in the online inductance identification, which can be expressed in several forms, such as in *dq*-axes and *αβ*-axes. The inductance can be calculated using these equations under changing operating conditions [43-44]. However, rank deficiency is an essential problem that must be solved [45-46]. In addition, cross-coupling exists between the parameters. Considering the *dq*-axes voltage equation as an example, it can be expressed as

$$\begin{cases} u_d = R_s i_d - \omega_e L_{q\_app} i_q \\ u_q = R_s i_q + \omega_e L_{d\_app} i_d + \omega_e \psi_f \end{cases} \tag{6}$$

As the parameters are contained in multiple components, the working conditions restrict the application of these identification methods. Meanwhile, the identification error of one parameter affects the identification accuracy of the other parameters, owing to parameter coupling. Several schemes have been proposed to address this problem.

3.2.1.1 Rank reduction strategy for identification method

The most intuitive method for reducing the rank of the voltage equations is to fix several other parameters in the equations until a full rank is achieved. The most commonly applied strategy for full-rank inductance identification is to assume constant resistance and flux linkage [47]. An adaptive synchronization-based inductance identification method is proposed considering the torque equation, where the moment of inertia and flux linkage are assumed to be constant [48]. The resistance was obtained separately to deal with the rank deficiency, and the identification error was limited to within 0.14% [49]. A flux-linkage-free method was proposed to make the model full rank, the identification error of which was within 1% [50]. However, the parameters change with the operating conditions, which should be considered in inductance identification [51-53].

To address the above problems, an identification strategy based on two recursive least square (RLS) algorithm segments of the fast- and slow-changing parameters with the current [54-55]. The identification model can be of full rank, and the inductance identification error can be limited to within 2% [7]. To further improve the effectiveness of RLS-based inductance methods, optimization algorithms such as the averaged sliding window and extended Kalman filter have been applied to reduce the disturbance influence during the identification process [56-58]. However, the inaccuracy caused by rank deficiency cannot be solved thoroughly.

The identification accuracy under rank deficiency can be improved to some extent by fixing or classifying the parameters based on fast or slow changing rates. However, these strategies cannot fully consider the inductance variation under different saturation conditions. Meanwhile, the rank deficiency amplifies the identification error, particularly under current disturbances caused by the pulsation error, system delay, and inverter nonlinearity effects. As a result, identification errors are also evident under transient operating conditions [59-60].

3.2.1.2 Full rank model using signal injection

Unlike the rank reduction strategy, the increase in the voltage equations by signal injection is another method that deals with the rank deficiency [43-45], the diagram of which is shown in Fig. 7. An inductance identification algorithm based on the *d*-axis current offset injection was proposed to develop another set of voltage equations, so that the entire voltage equation-based model is considered full rank, where the inductance identification error is less than 4% [44, 61-62]. In Ref. [63], a *q*-axis current injection was adopted, and the identification error was less than 10%. In Ref. [64], an HF square-wave voltage injection was used and the identification error was limited to 9.8%.

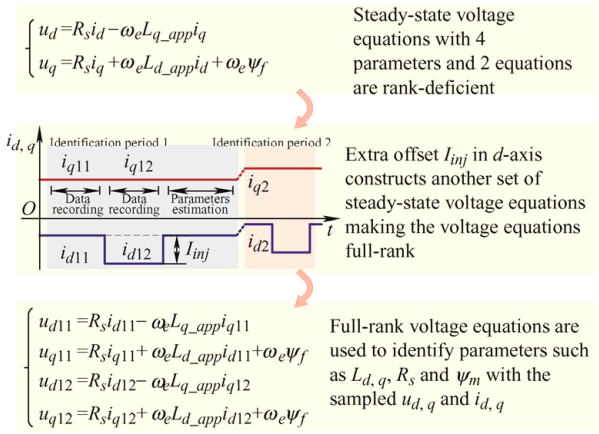

Fig. 7 Logic diagram of steady-state voltage-equation-based methods with signal injection

Because the injected current bias affects the saturation condition, the amplitude of the injected current should be set to a small value to reduce the negative effects [57]. However, owing to changes in the temperature and saturation effects, the parameters are not constant, making the above algorithms inaccurate. To further analyze the effect of the injected signal on the inductance identification, a linear equation was employed to simulate the saturation effect during current injection, which can facilitate the estimation of inductance variations induced by magnetic

saturation [65]. However, the nonlinear characteristics of inductance cannot be fully considered. Hence, the effect of the injected signal on the inductance requires further research and consideration [19].

3.2.1.3 Artificial intelligence methods

In recent years, artificial intelligence (AI) algorithms have been studied to optimize the efficiency of inductance identification methods [52]. AI algorithms can deal with a large amount of nonlinear data with autotuning functions and can also be trained to simulate unknown mathematical models under complex operating conditions. In Ref. [66], an artificial-neural-network-based high-performance speed control system for PMSM was proposed. In Ref. [67], an immune clonal selection differential evolution algorithm was applied for inductance identification. In Ref. [68], the genetic algorithm was studied for the parameter identification process of a PMSM under information interference conditions.

In addition to inductance identification, AI-based algorithms can consider the PMSM states. In Ref. [69], a particle swarm optimization algorithm (PSO) was implemented to estimate the parameters, considering the effect of temperature on the PMSM parameters. To further improve the convergence speed of the proposed method under different operating conditions, AI-based algorithms can achieve good convergence of the inductance, considering its nonlinear characteristics. However, these algorithms are still based on voltage equations, which are inevitably affected by the aforementioned problems of voltage equation models. However, AI-based methods are generally complex and time-consuming, which limits their application.

3.2.2 Transient-state voltage equation based methods

Although steady-state voltage-equation-based methods have made great progress in inductance identification, several problems, such as rank deficiency and coupling between parameters, remain [10]. Hence, the identified inductance is affected by possible errors of other parameters, such as sampling and perturbation errors. In this case, steady-state voltage equation-based methods cannot guarantee identification accuracy under full operating conditions.

Recently, inductance identification methods based on transient-state voltage equation have been investigated to address these issues [70]. A detailed comparison of the steady-and transient-state voltage equation-based methods is presented in Tab. 3.

Tab. 3 Comparison of steady- and transient-state voltage equation based online inductance identification methods

Contrastive items	Steady-state voltage equation based method	Transient-state voltage equation based method
Physical model	Fundamental frequency model	HF equivalent impedance model
Injected signal type	Square wave/offset signal injection	HF Sine wave signal injection
Application limitation	Inapplicable to specific conditions	Applicable to all working conditions
Application robustness	Affected by parameter coupling error	Not affected by the parameter coupling error

In these methods, HF signal injection is necessary, and incremental inductance is obtained. As the frequency of the injected HF signal is generally much higher than the motor speed, the transient components are also larger than the steady components. To simplify the calculation, steady parts were ignored. The mathematical formulas and diagrams of the methods are presented in Eq. (7) and Fig. 8.

$$\begin{cases} u_{xh} \approx L_{x\_inc}\mathrm{d}i_x / \mathrm{d}t \\ L_{x\_inc} = U_{xh}\sin(\theta_{ux} - \theta_{ix}) / \omega_x I_{xh} \end{cases} \quad x = d, q \tag{7}$$

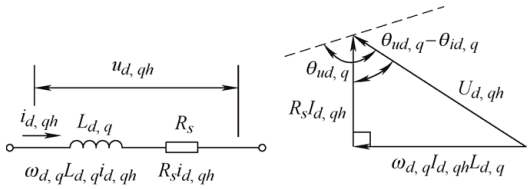

(a) Physical model (b) Vector form of model

Fig. 8 Diagram of PMSM transient model

As shown in Fig. 9, an HF equivalent impedance model based on the transient-state voltage equation was proposed in Ref. [10], in which the inductance was calculated using sine signal injection. In Ref. [18], the HF sinusoidal voltages are imposed on the $\alpha\beta$-axis to identify the d- and q-axis inductances. In Ref. [63], the difference between the incremental inductance and apparent inductance was discussed in detail using the proposed HF model. In Ref. [64], an HF square injection-based identification method was proposed, where the inductance can be calculated by the amplitudes of different sequence components in the HF current obtained by a fast Fourier transform (FFT). Except for signal injection, the harmonics of the pulse-width modulation excitation or current ripples can be directly used for inductance identification [71-73].

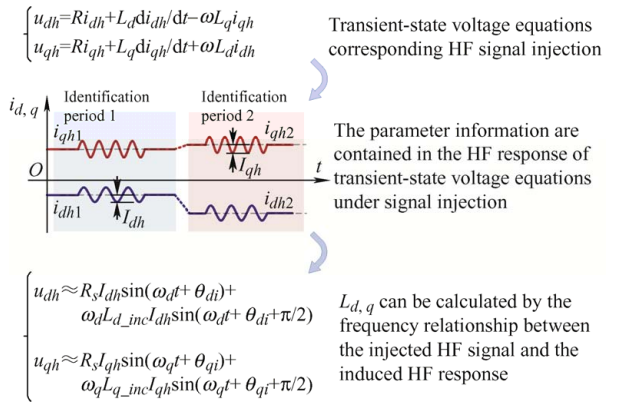

Fig. 9 Logic diagram of transient-state voltage-equation-based methods with signal injection

Compared with steady-state voltage equation-based methods, transient-state voltage equation-based methods have advantages in solving the rank deficiency problem and coupling effect because the HF transient-state model is independent of the PMSM operation conditions. This method is immune to inverter nonlinearity by avoiding the influence of the equivalent resistance. In conclusion, the transient-state voltage-equation-based methods expand the application of parameter identification. Using the transient-state voltage equation-based method, the identification error can be limited to within 5% and 6% for *dq*-axis inductance, respectively [10]. However, using steady-state voltage equation-based methods, the identification errors were 10% and 9.8% for Ref. [63] and Ref. [64], respectively.

4 Inverter nonlinearity self-learning and compensation of VSI-based inverter

Inverter nonlinearity is a crucial source of errors in inductance identification. This section reviews inverter nonlinearity compensation and self-learning methods.

4.1 Inverter nonlinearity compensation

The inverter nonlinearity consists of many parts, such as the dead-time effect, parasitic capacitance effect, and voltage drop of the switching devices. As the main part of inverter nonlinearity in the high-current region, the dead-time effect has been widely analyzed [74-75]. The dead-time effect can be easily compensated for by the sign function related to three-phase currents [40, 44, 65]. To improve the compensation accuracy, other inverter nonlinearity effects should also be compensated. The parameter function of the inverter nonlinearity is introduced, which can theoretically provide an accurate description of the inverter nonlinearity effects [76]. Hence, the parameter function can effectively improve the accuracy of the inverter nonlinearity compensation [77]. However, parameter-function-based compensated methods require inverter parameters, which reduces the universality of this method.

$$\begin{cases} u_{abcinv}(i_{abc})=C_{dq0\to abc}u_{dq0inv}(i_{abc})=C_{\alpha\beta0\to abc}u_{\alpha\beta0inv}(i_{abc}) \\ T_{abcinv}(i_{abc})=u_{abcinv}(i_{abc})T_s/U_{dc} \end{cases} \tag{8}$$

where u_{dq0inv} and $u_{\alpha\beta0inv}$ denote the inverter nonlinearity of $dq0$-axes and $\alpha\beta0$-axes. $C_{dq0\to abc}$ denotes the coordinate transformation matrices between *abc*-phases and $dq0$-axes. $C_{\alpha\beta0\to abc}$ denotes the coordinate transformation matrix between $\alpha\beta0$-axes and dq-axes. T_s denotes the PWM period. U_{dc} indicates the DC bus voltage. T_{abcinv} represents the equivalent dead time compensation.

To further improve the accuracy of the inverter nonlinearity compensation, the parasitic capacitance effect should be carefully considered [21, 78]. The characteristics of the parasitic capacitance effects of power-switching devices have been analyzed [23, 79]. Moreover, it was proven that the parasitic capacitance mainly affected the three-phase current-switching process. The equivalent voltage error of the parasitic capacitance effect and its relationship with the dead-time effect were introduced using the corresponding mathematical relationship [78]. To address the parasitic capacitance in the inverter nonlinearity effect, a compensation method based on a trapezoidal voltage was proposed, which improves the compensation effect in a relatively small current range [80-81]. In this method, the nonlinear inverter voltage error is equivalent to the slope function in the low-current region, which can be described by minimizing the current harmonics through a fast Fourier transform [24].

To better describe the parasitic capacitance effect in inductance identification in the low-current region, a two-stage inverter nonlinear voltage error fitting method based on the *d*-axis ramp current injection was proposed for inverter nonlinear compensation [41]. A method based on a detailed physical model of a power converter was introduced using a small set of parameters, based on which an identification self-commissioning procedure adopting multiple linear regression was proposed [21]. The application of the inverter nonlinearity compensation method is illustrated in Fig. 10.

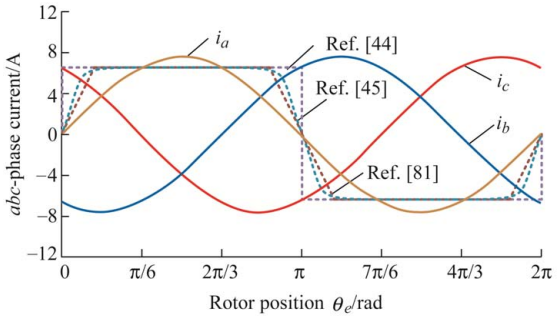

Fig. 10 Waveforms of several common inverter nonlinear compensation methods

4.2 Inverter nonlinearity self-learning

The sign function cannot describe the inverter nonlinearity characteristics in every aspect [2]. This parameter function is widely applicable to various controllers. Hence, in recent years, inverter nonlinearity self-learning methods have been studied. A self-learning scheme based on a double second-order generalized integrator frequency-locked loop was proposed to achieve adaptive compensation for the dead-zone effect and minimize current zero-crossing distortion [75]. An inverter output voltage error compensation method was introduced in which the harmonic component of the current in the synchronous rotating reference frame can be minimized [82]. An online inverter nonlinearity effect post-compensation scheme in a signal-injection-based sensor-less method was developed by utilizing the information of the positive-sequence carrier current distortion [76].

As illustrated in Fig. 11, the offline inverter nonlinearity self-learning method has been commonly applied [81, 83], in which the inverter nonlinearity characteristics under different currents should be considered. The inverter nonlinearity error can be measured directly by detecting the inverter nonlinearity voltage error [84]. Since the application of the test device increases the consumption, inverter nonlinearity self-learning methods based on signal injection have been investigated. In Ref. [41], a *d*-axis current-injection-based inverter nonlinearity self-learning method was investigated, and the inverter nonlinearity voltage error under different currents was obtained. In Ref. [85], the α-axis DC current injection based characterization algorithm was proposed for the inverter nonlinearity compensation, which realizes the self-commissioning of VSI-fed drives without numerical solutions. Meanwhile, an offline inverter nonlinearity self-learning method based on *a*- and *b*-phase current injection (*c*-phase disconnected) was studied [86]. In the offline self-learning process, a combination of the identified voltage error and current information was sampled and stored in a lookup table. The error voltage of the three-phase inverter can then be obtained through a coordinate transformation. Compensation can be achieved using real-time PMSM control [41].

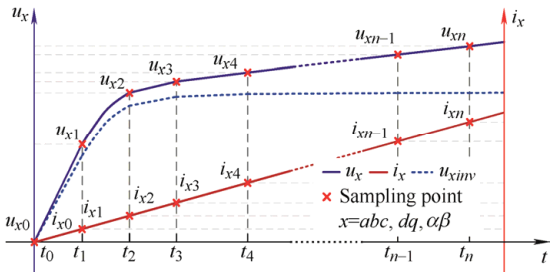

Fig. 11 Diagram of the inverter nonlinearity self-learning process with signal injection

However, existing methods can only be applied under specific rotor positions, which reduces the generality of the algorithm. To further improve its application and accuracy, an inverter nonlinear self-learning method that considers the zero-sequence voltage error was studied in Ref. [14], as shown in Fig. 12. Through offline inverter nonlinear self-learning, the nonlinear characteristics of the inverter can be considered to improve its accuracy and versatility. Nonlinear inverter self-learning strategies have been used in applications such as three-level T-type inverters [87], multi-level inverters [88], and inverters

with faulty units [85].

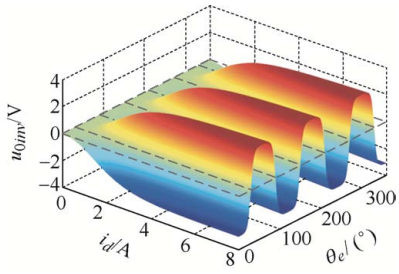

Fig. 12 Zero-sequence inverter nonlinearity voltage error versus current and rotor positions

5 Conclusions

This paper presented a detailed overview of inductance identification methods for PMSM drives. The methods were classified based on their application models and algorithms for effective understanding of the readers. Furthermore, inverter nonlinearity self-learning methods, which are important error sources in inductance identification, were reviewed.

However, significant progress has been made in the inductance identification techniques for PMSMs. To improve its effectiveness further, there are several aspects concerning future research trends in inductance identification.

(1) Conventional identification methods mostly consider the *dq*-axis self-inductance. The identification of PMSM mutual inductance should be further investigated.

(2) Since inductance identification methods still rely on signal injection, the effects of the injected signals on the identification and operation conditions need to be further studied.

(3) In actual machine control, the values of the incremental inductance and apparent inductance are not equal, which should be considered in PMSM control.

(4) An effective control algorithm upgrade based on the identified inductances and inverter nonlinearity information should be investigated.

References

[1] Y Zhang, L Huang, D Xu, et al. Performance evaluation of two-vector-based model predictive current control of PMSM drives. *Chinese Journal of Electrical Engineering*, 2018, 4(2): 65-81.

[2] Q Wang, G Zhang, G Wang, et al. Offline parameter self-learning method for general-purpose PMSM drives with estimation error compensation. *IEEE Transactions on Power Electronics*, 2019, 34(11): 11103-11115.

[3] M S Rafaq, J Jung. A comprehensive review of state-of-the-art parameter estimation techniques for permanent magnet synchronous motors in wide speed range. *IEEE Transactions on Industrial Informatics*, 2020, 16(7): 4747-4758.

[4] Y Hu, W Hua, M Hu, et al. Inductance-resistance online identification for sensorless high-speed PMSM considering resistive characteristic of invertor nonlinearity. *IEEE Transactions on Industrial Electronics*, 2024, 71(3): 2343-2355.

[5] H Yang, Y Zhang, N Zhang, et al. A voltage sensorless finite control set-model predictive control for three-phase voltage source PWM rectifiers. *Chinese Journal of Electrical Engineering*, 2016, 2(2): 52-59.

[6] Z Wang, J Chai, X Sun. A novel online parameter identification algorithm for deadbeat control of PMSM drive. *IEEE 3rd Student Conference on Electrical Machines and Systems*, 2020: 769-774.

[7] K Yin, L Gao, W Fu, et al. Deadbeat predictive current control of PMSM with nonlinear parameters online identification. *IEEE 4th International Conference on Electronics Technology*, 2021: 138-142.

[8] D Wen, J Yuan, Y Zhang, et al. Improved optimal duty model predictive current control strategy for PMSM. *Chinese Journal of Electrical Engineering*, 2022, 8(3): 133-141.

[9] A Brosch, O Wallscheid, J Böcker. Torque and inductances estimation for finite model predictive control of highly utilized permanent magnet synchronous motors. *IEEE Transactions on Industrial Informatics*, 2021, 17(12): 8080-8091.

[10] Q Wang, G Wang, N Zhao, et al. An impedance model-based multiparameter identification method of PMSM for both offline and online conditions. *IEEE Transactions on Power Electronics*, 2021, 36(1): 727-738.

[11] R Ni, D Xu, G Wang, et al. Maximum efficiency per ampere control of permanent magnet synchronous machines. *IEEE Transactions on Industrial Electronics*, 2015, 62(4): 2135-2143.

[12] J Lee, H Seo, J S Lee, et al. Electrical parameter

estimation method for surface-mounted permanent magnet synchronous motors considering voltage source inverter nonlinearity. *IEEE Access*, 2023, 11: 16288-16296.

[13] Z Li, G Feng, C Lai, et al. Current injection-based multi-parameter estimation for dual three-phase IPMSM considering VSI nonlinearity. *IEEE Transactions on Transportation Electrification*, 2019, 5(2): 405-415.

[14] Q Wang, S Liu, G Zhang, et al. Zero-sequence voltage error elimination based offline VSI nonlinearity identification for PMSM drives. *IEEE Transactions on Transportation Electrification*, doi: 10.1109/TTE.2023.3264527.

[15] Q Wang, N Zhao, G Wang, et al. An offline parameter self-learning method considering inverter nonlinearity with zero-axis voltage. *IEEE Transactions on Power Electronics*, 2021, 36(12): 14098-14109.

[16] G Pan, Q Wang, K Zhang, et al. Online inductance identification of PMSM based on HF signal injection into virtual axis. *25th International Conference on Electrical Machines and Systems*, 2022: 1-5.

[17] X Xiong, Q Wang, S Liu, et al. Online multi-parameter identification of PMSM based on HF equivalent impedance model. *25th International Conference on Electrical Machines and Systems*, 2022: 1-6.

[18] C Wu, Y Zhao, M Sun. Enhancing low-speed sensorless control of PMSM using phase voltage measurements and online multiple parameter identification. *IEEE Transactions on Power Electronics*, 2020, 35(10): 10700-10710.

[19] S M Seyyedzadeh, A Shoulaie. Accurate modeling of the nonlinear characteristic of a voltage source inverter for better performance in near zero currents. *IEEE Transactions on Industrial Electronics*, 2019, 66(1): 71-78.

[20] U Abronzini, C Attaianese, M D'Arpino, et al. Steady-state dead-time compensation in VSI. *IEEE Transactions on Industrial Electronics*, 2016, 63(9): 5858-5866.

[21] N Bedetti, S Calligaro, R Petrella. Self-commissioning of inverter deadtime compensation by multiple linear regression based on a physical model. *IEEE Transactions on Industry Applications*, 2015, 51(5): 3954-3964.

[22] Z Tang, B Akin. Suppression of dead-time distortion through revised repetitive controller in PMSM drives. *IEEE Transactions on Energy Conversion*, 2017, 32(3): 918-930.

[23] D Wang, P Zhang, Y Jin, et al. Influences on output distortion in voltage source inverter caused by power devices' parasitic capacitance. *IEEE Transactions on Power Electronics*, 2018, 33(5): 4261-4273.

[24] Y Park, S Sul. Implementation schemes to compensate for inverter nonlinearity based on trapezoidal voltage. *IEEE Transactions on Industry Applications*, 2014, 50(2): 1066-1073.

[25] G Feng, C Lai, W Li, et al. Efficient permanent magnet temperature modeling and estimation for dual three-phase PMSM considering inverter nonlinearity. *IEEE Transactions on Power Electronics*, 2020, 35(7): 7328-7340.

[26] G Wang, L Qu, H Zhan, et al. Self-commissioning of permanent magnet synchronous machine drives at standstill considering inverter nonlinearities. *IEEE Transactions on Power Electronics*, 2014, 29(12): 6615-6627.

[27] L Peretti, P Sandulescu, G Zanuso. Self-commissioning of flux linkage curves of synchronous reluctance machines in quasi-standstill condition. *IET Electric Power Applications*, 2015, 9(9): 642-651.

[28] M Hinkkanen, P Pescetto, E Mölsä, et al. Sensorless self-commissioning of synchronous reluctance motors at standstill without rotor locking. *IEEE Transactions on Industry Applications*, 2017, 53(3): 2120-2129.

[29] N Bedetti, S Calligaro, R Petrella. Stand-still self-identification of flux characteristics for synchronous reluctance machines using novel saturation approximating function and multiple linear regression. *IEEE Transactions on Industry Applications*, 2016, 52(4): 3083-3092.

[30] P Pescetto, G Pellegrino. Automatic tuning for sensorless commissioning of synchronous reluctance machines augmented with HF voltage injection. *IEEE Transactions on Industry Applications*, 2018, 54(5): 4485-4493.

[31] J Zhou, K Huang, S Huang, et al. Inductance parameter identification method of permanent magnet synchronous motor based on the HF rotating square wave voltage injection. *22nd International Conference on Electrical Machines and Systems*, 2019: 1-4.

[32] X Wu, X Fu, M Lin, et al. Offline inductance

identification of IPMSM with sequence-pulse injection. *IEEE Transactions on Industrial Informatics*, 2019, 15(11): 6127-6135.

[33] S A Odhano, R Bojoi, Ş G Roşu, et al. Identification of the magnetic model of permanent-magnet synchronous machines using DC-biased low-frequency AC signal injection. *IEEE Transactions on Industry Applications*, 2015, 51(4): 3208-3215.

[34] S A Odhano, P Giangrande, R I Bojoi, et al. Self-commissioning of interior permanent-magnet synchronous motor drives with HF current injection. *IEEE Transactions on Industry Applications*, 2014, 50(5): 3295-3303.

[35] J Long, M Yang, Y Chen, et al. Current-controller-free self-commissioning scheme for deadbeat predictive control in parametric uncertain SPMSM. *IEEE Access*, 2021, 9: 289-302.

[36] F Erturk, B Akin. Spatial inductance estimation for current loop auto-tuning in IPMSM self-commissioning. *IEEE Transactions on Industrial Electronics*, 2020, 67(5): 3911-3920.

[37] C Li, G Wang, G Zhang, et al. Saliency-based sensorless control for SynRM drives with suppression of position estimation error. *IEEE Transactions on Industrial Electronics*, 2019, 66(8): 5839-5849.

[38] Q Wang, G Wang, S Liu, et al. An inverter-nonlinearity-immune offline inductance identification method for PMSM drives based on equivalent impedance model. *IEEE Transactions on Power Electronics*, 2022, 37(6): 7100-7112.

[39] G Pellegrino, B Boazzo, T M Jahns. Magnetic model self-identification for PM synchronous machine drives. *IEEE Transactions on Industry Applications*, 2015, 51(3): 2246-2254.

[40] K Liu, Z Q Zhu. Position offset-based parameter estimation for permanent magnet synchronous machines under variable speed control. *IEEE Transactions on Power Electronics*, 2015, 30(6): 3438-3446.

[41] G Wang, Y Wang, J Qi, et al. Offline inductance identification of PMSM with adaptive inverter nonlinearity compensation. *9th International Conference on Power Electronics and ECCE Asia*, 2015: 2438-2444.

[42] C Lai, G Feng, Z Li, et al. Computation-efficient decoupled multiparameter estimation of PMSMs from massive redundant measurements. *IEEE Transactions on Power Electronics*, 2020, 35(10): 10729-10740.

[43] Z Liu, H Wei, Q Zhong, et al. GPU implementation of DPSO-RE algorithm for parameters identification of surface PMSM considering VSI nonlinearity. *IEEE Transactions on Power Electronics*, 2017, 5(3): 1334-1345.

[44] Z Liu, H Wei, Q Zhong, et al. Parameter estimation for VSI-fed PMSM based on a dynamic PSO with learning strategies. *IEEE Transactions on Power Electronics*, 2017, 32(4): 3154-3165.

[45] Z Liu, H Wei, X Li, et al. Global identification of electrical and mechanical parameters in PMSM drive based on dynamic self-learning PSO. *IEEE Transactions on Power Electronics*, 2018, 33(12): 10858-10871.

[46] K Liu, Z Q Zhu, D A Stone. Parameter estimation for condition monitoring of PMSM stator winding and rotor permanent magnets. *IEEE Transactions on Industrial Electronics*, 2013, 60(12): 5902-5913.

[47] M N Uddin, M M I Chy. Online parameter-estimation-based speed control of PM AC motor drive in flux-weakening region. *IEEE Transactions on Industry Applications*, 2008, 44(5): 1486-1494.

[48] L Liu, D A Cartes. Synchronisation based adaptive parameter identification for permanent magnet synchronous motors. *IET Control Theory & Applications*, 2007, 1(4): 1015-1022.

[49] T Hu, J Liu, J Cao, et al. On-line parameter identification of permanent magnet synchronous motor based on extended Kalman filter. *25th International Conference on Electrical Machines and Systems*, 2022: 1-6.

[50] S Zhao, X Huang, Q Hu, et al. Improved MRAS parameter identification method for PMSM based on permanent magnet flux linkage free model. *25th International Conference on Electrical Machines and Systems*, 2022: 1-4.

[51] A Brosch, O Wallscheid, J Böcker, et al. Long-term memory recursive least squares online identification of highly utilized permanent magnet synchronous motors for finite-control-set model predictive control. *IEEE Transactions on Power Electronics*, 2023, 38(2): 1451-1467.

[52] Z Ma, W Zhang, J He, et al. Multi-parameter online identification of permanent magnet synchronous motor based on dynamic forgetting factor recursive least squares. *IEEE 5th International Electrical and Energy Conference*,

2022: 4865-4870.

[53] G Feng, C Lai, X Tan, et al. Multi-parameter estimation of PMSM using differential model with core loss compensation. *IEEE Transactions on Transportation Electrification*, 2022, 8(1): 1105-1115.

[54] S J Underwood, I Husain. Online parameter estimation and adaptive control of permanent-magnet synchronous machines. *IEEE Transactions on Industrial Electronics*, 2010, 57(7): 2435-2443.

[55] Y Yu, X Huang, Z Li, et al. Full parameter estimation for permanent magnet synchronous motors. *IEEE Transactions on Industrial Electronics*, 2022, 69(5): 4376-4386.

[56] Q Liu, K Hameyer. A fast online full parameter estimation of a PMSM with sinusoidal signal injection. *IEEE Energy Conversion Congress and Exposition*, 2015: 4091-4096.

[57] H Li, T Chen, H Yao. The full rank identification of PM flux linkage for PMSM. *IEEE 8th International Power Electronics and Motion Control Conference*, 2016: 2993-2998.

[58] X Li, R Kennel. General formulation of Kalman-filter-based online parameter identification methods for VSI-fed PMSM. *IEEE Transactions on Industrial Electronics*, 2021, 68(4): 2856-2864.

[59] S Ichikawa, M Tomita, S Doki. Sensorless control of permanent-magnet synchronous motors using online parameter identification based on system identification theory. *Electrical Engineering*, 2006, 53(2): 363-372.

[60] S Moreau, R Kahoul. Parameters estimation of permanent magnet synchronous machine without adding extra-signal as input excitation. *IEEE International Symposium on IEEE*, 2006: 1-5.

[61] J Jiang, Z Zhang. Multi-parameter identification of permanent magnet synchronous motor based on improved grey wolf optimization algorithm. *IEEE 4th Student Conference on Electric Machines and Systems*, 2021: 1-7.

[62] W Feng, W Zhang, S Huang. A novel parameter estimation method for PMSM by using chaotic particle Swarm optimization with dynamic self-optimization. *IEEE Transactions on Vehicular Technology*, 2023, 72(7): 8424-8432.

[63] C Li, B Kudra, V Balaraj, et al. Absolute inductance estimation of PMSM considering HF resistance. *IEEE Transactions on Energy Conversion*, 2021, 36(1): 81-94.

[64] K Yu, Z Wang. Online decoupled multi-parameter identification of dual three-phase IPMSM under position-offset and HF signal injection. *IEEE Transactions on Industrial Electronics*, 2024, 71(4): 3429-3440.

[65] G Feng, C Lai, K Mukherjee, et al. Current injection-based online parameter and VSI nonlinearity estimation for PMSM drives using current and voltage DC components. *IEEE Transactions on Transportation Electrification*, 2016, 2(2): 119-128.

[66] R Kumar, R A Gupta, A K Bansal. Identification and control of PMSM using artificial neural network. *IEEE International Symposium on Industrial Electronics*, 2007: 30-35.

[67] G Lin, J Zhang, Z Liu. Parameter identification of PMSM using immune clonal selection differential evolution algorithm. *Mathematical Problems in Engineering*, 2014, 9(2014): 1-10.

[68] A Avdeev, O Osipov. PMSM identification using genetic algorithm. *International Workshop on Electric Drives: Improvement in Efficiency of Electric Drives*, 2019: 1-4.

[69] E M Tofighi, A Mahdizadeh, M R Feyzi. Real time estimation and tracking of parameters in permanent magnet synchronous motor using a modified two stage particle swarm optimization algorithm. *IEEE International Symposium on Sensorless Control for Electrical Drives and Predictive Control of Electrical Drives and Power Electronics*, 2013: 1-7.

[70] T Liu, C Wang, Y Hu, et al. Offline inductance identification of PMSM using HF current signal injection. *22nd International Conference on Electrical Machines and Systems*, 2019: 1-8.

[71] R Raja, T Sebastian, M Wang. Online stator inductance estimation for permanent magnet motors using PWM excitation. *IEEE Transactions on Transportation Electrification*, 2019, 5(1): 107-117.

[72] J Zhang, F Peng, Y Huang, et al. Online inductance identification using PWM current ripple for position sensorless drive of high-speed surface-mounted permanent magnet synchronous machines. *IEEE Transactions on Industrial Electronics*, 2022, 69(12): 12426-12436.

[73] K Choi, Y Kim, K S Kim, et al. Using the stator current ripple model for real-time estimation of full parameters of a permanent magnet synchronous motor. *IEEE Access*, 2019, 7: 33369-33379.

[74] Z Shen, D Jiang. Dead-time effect compensation method based on current ripple prediction for voltage-source inverters. *IEEE Transactions on Power Electronics*, 2019, 34(1): 971-983.

[75] Q Yan, R Zhao, X Yuan, et al. A DSOGI-FLL-based dead-time elimination PWM for three-phase power converters. *IEEE Transactions on Power Electronics*, 2019, 34(3): 2805-2818.

[76] L M Gong, Z Q Zhu. A novel method for compensating inverter nonlinearity effects in carrier signal injection-based sensorless control from positive sequence carrier current distortion. *IEEE Transactions on Industry Applications*, 2011, 47(3): 1283-1292.

[77] M Gong, Z Q Zhu. Modeling and compensation of inverter nonlinearity effects in carrier signal injection-based sensorless control methods from positive sequence carrier current distortion. *2010 IEEE Energy Conversion Congress and Exposition*, 2010: 3434-3441.

[78] Z Zhang, L Xu. Dead-time compensation of inverters considering snubber and parasitic capacitance. *IEEE Transactions on Power Electronics*, 2014, 29(6): 3179-3187.

[79] F Chierchie, E E Paolini, L Stefanazzi. Dead-time distortion shaping. *IEEE Transactions on Power Electronics*, 2019, 34(1): 53-63.

[80] Y Park, S K Sul. A novel method utilizing trapezoidal voltage to compensate for inverter nonlinearity. *IEEE Transactions on Power Electronics*, 2012, 27(12): 4837-4846.

[81] M El-daleel, A Mahgoub. Accurate and simple improved lookup table compensation for inverter dead time and nonlinearity compensation. *19th International Middle East Power Systems Conference*, 2017: 1358-1361.

[82] H Zhao, Q M J Wu, A Kawamura. An accurate approach of nonlinearity compensation for VSI inverter output voltage. *IEEE Transactions on Power Electronics*, 2004, 19(4): 1029-1035.

[83] G Shen, W Yao, B Chen, et al. Auto measurement of the inverter output voltage delay curve to compensate for inverter nonlinearity in sensorless motor drives. *IEEE Transactions on Power Electronics*, 2014, 29(10): 5542-5553.

[84] A S Babel, A Muetze, R R Seebacher, et al. Inverter device nonlinearity characterization technique for use in a motor drive system. *IEEE Transactions on Industry Applications*, 2015, 51(3): 2331-2339.

[85] S M Seyyedzadeh, S Mohamadian, M Siami, et al. Modeling of nonlinear characteristics of voltage source inverters for motor self-commissioning. *IEEE Transactions on Power Electronics*, 2019, 34(12): 12154-12164

[86] X Wang, S Nalakath, S Filho, et al. A simple and effective compensation method for inverter nonlinearity. *2020 IEEE Transportation Electrification Conference & Expo*, June 23-26, 2020, Chicago, IL, USA. IEEE, 2020: 638-643.

[87] H Kim, Y Kwon, S Chee, et al. Analysis and compensation of inverter nonlinearity for three-level T-type inverters. *IEEE Transactions on Power Electronics*, 2017, 32(6): 4970-4980.

[88] B Chen, Y Chen, C Tian, et al. Analysis and suppression of circulating harmonic currents in modular multilevel converter considering the impact of dead time. *IEEE Transactions on Power Electronics*, 2015, 30(7): 3542-3552.

Qiwei Wang received the B.S., M.S., and Ph.D. degrees in Electrical Engineering from the Harbin Institute of Technology, Harbin, China, in 2015, 2017, and 2022, respectively. He is currently working as a Postdoc in Power Electronics and Electrical Drives with the School of Electrical Engineering and Automation.

His research interests include parameter identification technique, position sensorless control and model prediction control.

Jiqing Xue received the B.S. degrees in Electrical Engineering from the Harbin Institute of Technology, Harbin, China, in 2022. He is currently working toward the Ph.D. degree in Power Electronics and Electrical Drives at the Harbin Institute of Technology, Harbin, China.

His current research interests include PMSM parameter identification technique and model prediction control.

Gaolin Wang (Senior Member, IEEE) received the B.S., M.S., and Ph.D. degrees in Electrical Engineering from the Harbin Institute of Technology (HIT), Harbin, China, in 2002, 2004, and 2008, respectively. In 2009, he joined the Department of Electrical Engineering, HIT, as a Lecturer, where he has been a Full Professor of Electrical Engineering, since 2014. He has authored more than 70 technical papers published in IEEE Transactions.

His research interests include permanent magnet synchronous motor drives and power converters. Prof. Wang serves as a Guest Associate Editor of IEEE Transactions on Industrial Electronics, and an Associate

Editor of IEEE Transactions on Transportation Electrification and IET Electric Power Applications.

Yihua Hu (Senior Member, IEEE) received the B.S. degree in Electrical Engineering in 2003 and the Ph.D. degree in Power Electronics and Drives in 2011, both from the China University of Mining and Technology. Between 2013 and 2015, he was a Research Associate with the Power Electronics and Motor Drive Group, University of Strathclyde, UK. He is currently a Reader with the Department of Engineering, King's College London, UK.

His research interests include renewable generation, power electronics converters and control, electric vehicle, more electric ship/aircraft, smart energy system and non-destructive test technology. He was the recipient of Royal Society Industry Fellowship. He is the Fellow of Institution of Engineering and Technology (FIET) and a Member of UK Young Academy.

Dianguo Xu (Fellow, IEEE) received the B.S. degree in Control Engineering from the Harbin Engineering University, Harbin, China, in 1982, and the M.S. and the Ph.D. degrees in Electrical Engineering from the Harbin Institute of Technology (HIT), Harbin, China, in 1984 and 1989, respectively.

In 1984, he was an Assistant Professor with the Department of Electrical Engineering, HIT. Since 1994, he has been a Professor with the Department of Electrical Engineering, HIT. He was the Dean of the School of Electrical Engineering and Automation, HIT, from 2000 to 2010. He was the Vice President of the HIT, from 2014 to 2020. He has authored or coauthored more than 600 technical papers. His research interests include motor drives, PMSM servo drives, renewable energy generation technology, etc.

Prof. Xu serves as the Co-EIC for IEEE Transactions on Power Electronics, and an Associate Editor for IEEE Transactions on Industrial Electronics and IEEE Journal of Emerging and Selected Topics in Power Electronics.